Correlating surface structure and electrochemical properties of polycrystalline platinum electrodes

Fröhlich, N.L.; Sjö, H.; Mascaró, F.V.; Koper, M.T.M.

Electrochimica Acta 548 (2026) 147977

Contents lists available at ScienceDirect

Electrochimica Acta

journal homepage: www.journals.elsevier.com/electrochimica-acta

Correlating surface structure and electrochemical properties of polycrystalline platinum electrodes

Nicci L. Fröhlich [a], Hanna Sjö [b], Francesc Valls Mascaró [c], Marc T.M. Koper [a,*]

[a] Leiden Institute of Chemistry, Leiden University, Einsteinweg 55, 2333 CC Leiden, the Netherlands
[b] Department Physics, Lund University, Box 118, 221 00, Lund, Sweden
[c] Department of Physical Chemistry, University of Innsbruck, Innrain 52c, 6020 Innsbruck, Austria

ARTICLE INFO

Keywords:
Platinum
Polycrystalline
Double layer
Pseudocapacitance
EBSD

ABSTRACT

Platinum electrodes are of key importance in electrocatalysis due to their high activity for the hydrogen evolution and oxygen reduction reactions. Industrially-relevant Pt electrodes typically exhibit significant surface heterogeneity (*i.e.*, poly-/nanocrystallinity), complicating the establishment of clear relationships between structure and electrochemical properties. To unravel the influence of surface structure on interfacial properties at a fundamental level, two key electrochemical parameters are studied here: the potential of zero total charge (E_{pztc}) and the "double-layer" capacity (C_{dl}). Using a combination of cyclic voltammetry, electrochemical impedance spectroscopy, and *ex situ* electron backscatter diffraction, the electrochemical responses of three different polycrystalline Pt electrodes are compared and correlated with their respective facet orientation distributions. We show that, despite significant surface complexity, the E_{pztc} and C_{dl} remain highly sensitive to local facet orientations, mirroring trends previously observed for model stepped single-crystal Pt surfaces. In particular, (100)-type sites dominate the capacitance response in the so-called "double-layer" region (between 0.40 – 0.60 V_{RHE}), due to pseudocapacitive contributions resulting from a potential-dependent OH_{ads} coverage. These findings confirm that the structure-sensitivity of electrochemical properties previously identified for model systems can be predictably extended to polycrystalline Pt electrodes and provides a fundamental insight into macroscopic electrochemical behavior based on microscopic surface features.

1. Introduction

Platinum electrodes are of significant interest due to their exceptional catalytic activity, particularly for the hydrogen evolution (HER) and oxygen reduction (ORR) reactions. However, industrially-relevant poly-/nanocrystalline Pt electrodes are inherently heterogeneous, comprising a mixture of crystallographic facet orientations, defect sites, and grain boundaries. This structural complexity convolutes structure-activity relationships, such that a precise fundamental understanding of the factors that govern the catalytic activity of Pt electrodes is difficult to establish [1–3].

A key step towards addressing this challenge is gaining a detailed understanding of the electrode-electrolyte interface (EEI), which has proven elusive even for model Pt electrodes. A critical parameter in this context is the potential of zero total charge, E_{pztc}, [4,5] which is defined as the potential at which double-layer charging exactly counterbalances the residual charge arising from chemisorbed species, *i.e.*, chemisorption is implicitly accounted for [6,7]. Previous studies employing model single-crystal electrodes and high-resolution techniques such as scanning electrochemical cell microscopy (SECCM) have revealed a direct, structure-sensitive correlation between ORR/HER activity and the E_{pztc}, highlighting the importance of this parameter [2,8–10]. However, these measurements were limited to complex, highly-specialised experimental setups, or microscopic Pt electrodes. Therefore, it would be of significant interest to investigate the influence of surface structure on the E_{pztc} of poly-/nanocrystalline Pt electrodes at a macroscopic scale. In this context, Feliu et al. pioneered the CO displacement method to determine the E_{pztc} for Pt electrodes [11,12]. Their work demonstrated that the E_{pztc} values of shape-controlled Pt nanoparticles directly correlates with their respective facet orientation distributions, where these distributions are directly reflected in the characteristic features of their corresponding blank voltammograms, in turn serving as structural "fingerprints" [1]. Therefore, this suggests that knowledge of the surface structure of the electrode and the corresponding E_{pztc} values of the Pt basal planes may

* Corresponding author.
E-mail address: m.koper@chem.leidenuniv.nl (M.T.M. Koper).

https://doi.org/10.1016/j.electacta.2025.147977
Received 13 November 2025; Received in revised form 5 December 2025; Accepted 7 December 2025
Available online 7 December 2025

be sufficient to accurately predict the overall E_{pztc} of higher index Pt surfaces, in spite of significant surface heterogeneity. We will investigate this hypothesis here.

In addition to the E_{pztc}, another key parameter for probing interfacial properties is the double-layer capacitance, C_{dl}, which, under ideally polarisable conditions, quantifies the potential-dependent ion arrangement at the EEI, in turn providing a direct insight into the electrical double-layer (EDL) structure [13]. It is well-established that Pt(111) is the only Pt facet for which a true double-layer window exists in the non-specifically adsorbing $HClO_4$ electrolyte (0.40 – 0.60 V_{RHE}) where the surface remains free of adsorbates [14]. This double-layer window is bordered by pseudocapacitive regions associated with the electrosorption of dissociated H_2O species, *i.e.*, hydrogen (H_{upd} region, 0.05 – 0.40 V_{RHE}) and hydroxyl species (OH_{ads} region, 0.60 – 0.85 V_{RHE}) [1]. Importantly, within the double-layer window, the Gouy-Chapman-predicted capacitance minimum at the potential of zero (free) charge can be directly observed for Pt(111), but only in extremely dilute electrolyte (*i.e.*, 0.1 mM $HClO_4$, pH 4, 0.54 V_{RHE}) [15,16].

In contrast to Pt(111), lower-coordinated Pt facets (*i.e.*, (110) and (100)) exhibit a greater affinity for H_2O dissociation such that, as hydrogen species are desorbed from the surface, hydroxyl species are simultaneously adsorbed and *vice versa* [17–19]. The result is that for all Pt surfaces other than Pt(111) in the double-layer window, no adsorbate-free potential window exists, *i.e.*, there is always some coverage of H_{ads} and/or OH_{ads}, and as a result the interface is pseudocapacitive. Therefore, we argue that for all Pt surfaces other than Pt (111), including polycrystalline Pt electrodes, [20] it would be more appropriate to refer to the double-layer window (*i.e.*, between 0.40 – 0.60 V_{RHE}) as the low capacitance region (LCR).

Understanding the potential-dependencies of this adsorbate exchange/coverage in a given potential window on Pt surfaces has important ramifications for interpreting the capacitance measured. Recently, we studied the EDL structure at model stepped single crystal Pt electrodes, where the effect of surface heterogeneity and the influence of different Pt facets was investigated systematically by introducing different densities of monoatomic (110)-/(100)-steps to a (111)-terraced surface [21]. This work revealed that the capacitance measured in the LCR of stepped Pt single crystal electrodes is extremely structure-sensitive: increasing with (100)-step density, but decreasing for (110)-type steps. The increase in capacitance in the LCR region for (100)-stepped surfaces was explained to result from a potential-dependent adsorbate coverage at the (100)-sites, in turn contributing an additional pseudo-(adsorption) capacitance that dominates the capacitance measured. Such a pseudo-(adsorption) capacitance is not observed for the (110)-stepped series as the OH_{ads} coverage on (110)-type steps in the LCR region is likely potential-independent. Importantly, it was therefore hypothesised that the large pseudo-(adsorption) capacitance associated with (100)-sites should generally dominate the total capacitance response in the LCR of Pt electrodes [21].

While stepped Pt single crystals serve as valuable model systems for probing structure-capacitance relationships, it remains essential to assess whether such insights extend beyond model systems to more industrially-relevant, heterogeneous surfaces. To this end, we investigate three polycrystalline Pt electrodes using cyclic voltammetry (CV), electrochemical impedance spectroscopy (EIS) and *ex situ* electron backscatter diffraction (EBSD, a scanning electron microscopy method), as complementary techniques for surface characterisation and the determination of their respective electrochemical properties. Despite structural complexity, we demonstrate a clear correlation between facet orientation distribution and fundamental electrochemical properties for these polycrystalline Pt electrodes: specifically, the "double-layer" capacity and E_{pztc}. These findings show that insights established from model single-crystal Pt surfaces remain applicable to more realistic, polycrystalline systems, thereby bridging the gap between fundamental studies and practical electrocatalytic applications.

2. Methods

2.1. Electrochemical measurement and cleaning procedure methods

The electrochemical cleaning of glassware, cyclic voltammetry (CV), electrochemical impedance spectroscopy (EIS) measurements and Ohmic drop compensation method employed in this study were performed following procedures outlined previously [16,22]. Three different polycrystalline Pt discs (poly_1 (dia. 3 mm), poly_2 (dia. 10 mm) and poly_3 (dia. 10 mm)) and single crystal Pt(111) (dia. 3 mm, MaTeck, 99.999 %), Pt(110) (dia. 4 mm, MaTeck, 99.999 %) and Pt (100) (dia. 4 mm, MaTeck, 99.999 %) were used as the working electrodes. All potentials in this manuscript are reported *versus* the reversible hydrogen electrode (RHE) scale and Ohmic drop-corrected appropriately. For additional information and justification of the parameters used in the CV and EIS measurements, see ref. 16. Diluted $HClO_4$ (60 % Merck Suprapur®) and H_2SO_4 (96 %, Suprapur®) electrolytes were pre-purged with Ar gas (Linde 5.0, ≥99.999 %) through polytetrafluoroethylene (PTFE) gas tubing to prevent O_2 permeation prior to electrochemical measurements. The CO displacement measurements were carried out in accordance with the method reported by Feliu et al. [11,12].

2.2. Electrode preparation procedure prior to electrochemical measurement

In the literature, a clean, reproducible polycrystalline Pt surface is typically prepared by electrochemical "activation" after mechanical polishing. This electrochemical "activation" involves oxidation–reduction cycling (ORCs) in H_2SO_4 electrolyte, which, in turn, eventually leads to a steady-state distribution of the different Pt facets, reflected in a stable "benchmark" CV [13,23]. However, this leads to significant surface roughening due to Pt oxidation and consequent structural transformations to the Pt surface which remain relatively unknown [24]. A clean Pt surface can also be prepared using the Clavilier method for Pt single crystals, [25,26] which involves first annealing and then cooling the electrode in a reductive atmosphere (typically either H_2, or CO). It should be noted that the annealing temperature is well below the melting point of Pt, meaning that the inherent polycrystalline nature of the Pt surface is not changed (*i.e.*, annealing in this context does not remove the grain boundaries intrinsic to the respective polycrystalline Pt electrode). Previous reports have suggested that annealing can have an effect on grain boundary size, but the reproducibility in the blank CVs between different annealing cycles suggests that this effect is negligibly small in this context [27]. Moreover, this single crystal preparation method results in a reproducible, clean Pt surface, as well as avoiding the need for electrochemical oxidative potentials (>0.6 V_{RHE}), such that no unknown structural transformations take place [20,24]. This method of surface preparation is also frequently used to avoid the formation of surface oxides and/or favour certain reconstructions in the case of the (110) facet and can also be employed in the case of these polycrystalline Pt electrodes [25,26,28,29]. Using this latter surface preparation method therefore allows for a better elucidation of the structure-activity relationships exhibited by these surfaces which are already complex due to surface heterogeneity, without the additional complication of surface restructuring. Therefore, all electrochemical measurements of these polycrystalline Pt electrodes (and of the single crystal Pt basal plane electrodes) were carried out after cooling in a H_2:Ar atmosphere as according to the Clavilier method [25,26] for preparing single crystal Pt electrodes and oxidative potentials were always avoided (*i.e.*, the upper vertex potential was limited to 0.60 V_{RHE}).

2.3. Electron backscatter diffraction (EBSD) measurement

The EBSD measurements were performed at the Department of

Geology at Lund University using an Oxford Instruments Symmetry S2 detector linked to a high-resolution field emission scanning electron microscope (FE-SEM; Tescan Mira3). The data was collected using Oxford Instruments AZtec software. The sample stage tilt relative to the detector was 70°. The scans were carried out using an accelerating voltage of 20 kV and 30 μm step size. The grain orientations were defined as the average orientation of a grain.

3. Results & discussion

Polycrystalline Pt electrodes are inherently heterogeneous, consisting of any proportion of defect and kink sites, grain boundaries, and grains terminated by different ratios of (111), (110) and (100) Pt facets (SI Fig. 1) [1]. To understand the correlation between surface structure and electrochemical properties, we determine the respective facet distributions of three different polycrystalline Pt electrodes (arbitrarily denoted as poly_1/2/3, respectively). Cyclic voltammetry (CV) carried out in H_2SO_4 electrolyte is commonly used for such (approximate) surface characterisation purposes, as the strong anion adsorption leads to three sharp, well-defined peaks in the hydrogen adsorption region, H_{ads}, at 0.13, 0.28 and 0.39 V. These peaks are typically attributed to adsorption on (110)-steps, (100)-steps and (100)-terraces, respectively, where the latter site ((100)-terraces) display an additional broad peak contribution (*ca.* 0.32 – 0.38 V, Fig. 1a) [30,31]. Contrastingly, hydrogen ad-/desorption on (111)-terraces results in a broad peak between 0 – 0.40 V, but remains obscured by the pseudocapacitance associated with the lower-coordinated (110)- and (100)-facets and non-trivialises the deconvolution of the charges in the H_{upd} region. Nevertheless, the relative charge under the pseudocapacitive peaks associated with (110)- and (100)-facets can be readily obtained and directly correlated to the proportion of these different Pt sites on a given polycrystalline Pt electrode [1,20].

It is also important to note that surface preparation and electrochemical treatment have a marked impact the resulting blank CV. In particular, the typical oxidation–reduction cycling (ORCs) treatment to clean polycrystalline Pt electrodes prior to electrochemical

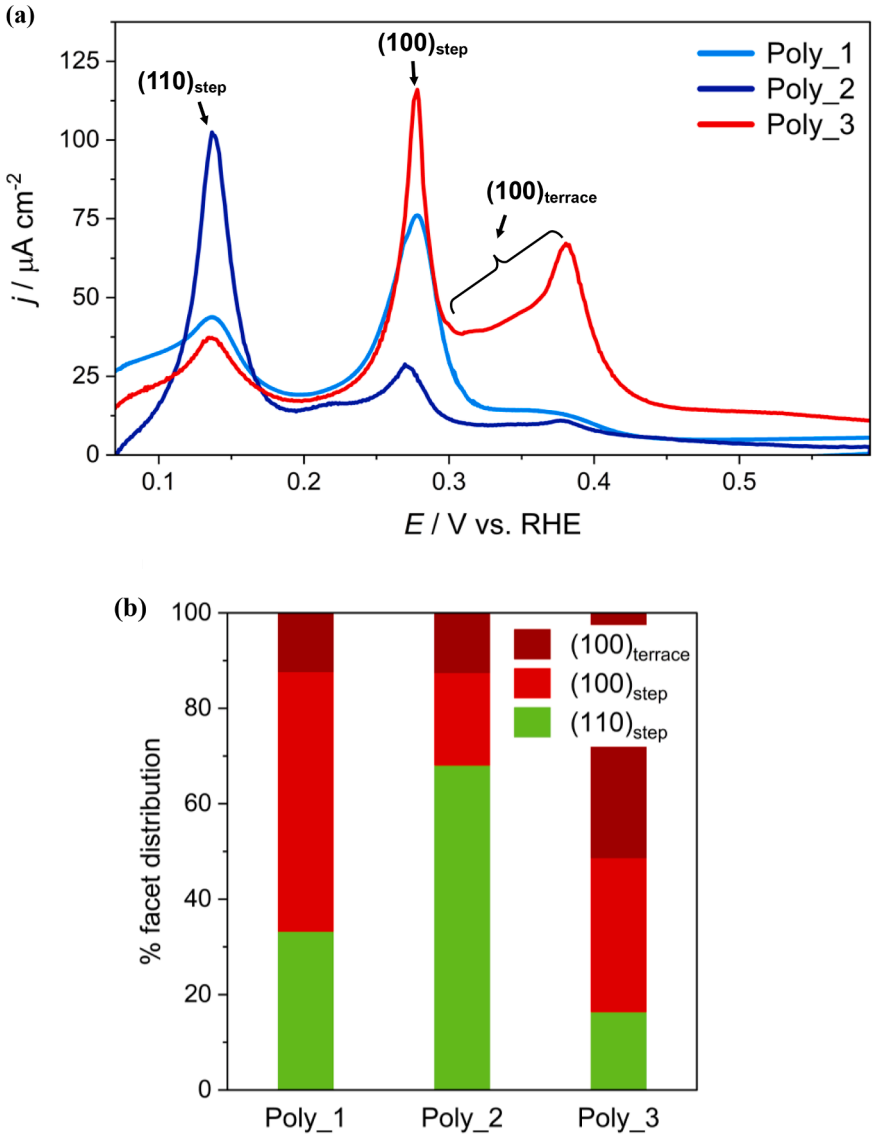

Fig. 1. (a) Positive-going H_{ads} region of CVs of three different polycrystalline Pt electrodes in 0.5 M H_2SO_4 when scanning between 0.07 – 0.60 V, $\nu = 50$ mV s^{-1} (see SI Fig. 2 for full CVs); (b) Proportion of (110)-step, (100)-step and (100)-terrace sites obtained by integral of fitted peaks in blank CVs of these corresponding polycrystalline Pt electrodes measured in 0.5 M H_2SO_4 using respective Lorentzian distribution functions. Note that these percentage facet distributions are approximate as an accurate estimation of the proportion of (111)-terrace sites cannot be obtained for polycrystalline Pt (see SI Fig. 3 for individual fits and further details).

measurement induce significant structural transformations, which are often ignored [13,23,24]. To avoid such complications, the polycrystalline Pt electrodes used here were prepared as according to the Clavilier method for single crystal Pt electrodes (annealing and cooling in a reductive atmosphere) [25,26] to achieve surface cleanliness without changing the surface structure inherent to the electrode and oxidative potentials were avoided (see Methods section for more details).

As shown in Fig. 1a, the hydrogen desorption region of the blank CVs of the three polycrystalline Pt electrodes differ markedly from one another (we note that these peaks do not involve only hydrogen desorption, but for convenience we sometimes refer to them as "hydrogen peaks") [18,19]. More specifically, the peaks at 0.13, 0.28 and 0.39 V – associated with (110)-steps, (100)-steps and (100)-terraces, respectively – arise from competitive anion and hydrogen ad- and desorption, reflected in a full-width at half maximum of < 90 mV [32]. Therefore, these peaks are most appropriately fitted with Lorentzian distribution functions (SI Fig. 3), enabling a quantitative assessment of the relative proportion of these lower-coordinated facets (Fig. 1b). It should be noted that the (100)-terrace peak was fitted with two respective Lorentzian distribution functions: one for the broader peak at more negative potentials (*i.e.*, between *ca.* 0.32 – 0.38 V), and one for the sharper peak at ~0.39 V (SI Fig. 3). Previous work on basal plane Pt (100) has strongly suggested that the former, broader (100)-terrace peak is related to the concurrent exchange of H_{ads} and OH_{ads} on two-dimensional (100)-sites, whereas the latter, sharper (100)-terrace peak is related to the exchange of OH_{ads} and the strongly-specifically adsorbing sulphate anion [33].

Consistent with the qualitative differences observed in the blank CVs (Fig. 1a), the quantitative peak fitting analysis (Fig. 1b) reveals that poly_1 and poly_3 contain greater proportions of (100)-sites (~65 and 85 %, respectively), although the ratio of (100)-step to (100)-terrace is much larger for poly_1 compared to poly_3. On the other hand, poly_2 is primarily constituted of (110)-steps (~70 %). However, as mentioned previously, the accurate quantification of the proportion of (111)-terrace sites using such a peak fitting analysis is challenging for polycrystalline Pt electrodes because the charge associated with hydrogen desorption on (111)-terrace sites remains convoluted underneath the large pseudocapacitance contributed by the lower-coordinated facets in the same potential window [32,34]. To address this, we used *ex situ* electron backscatter diffraction (EBSD) as a complementary, surface-sensitive technique that enables the determination of the facet orientation of each grain (Fig. 2). In turn, EBSD allows for a more complete overview of the facet distributions present on these three polycrystalline Pt electrodes (including those of (111)-nature) compared to CV analysis.

As shown in Fig. 2, very few of the grains are perfectly (111), (110), or (100) in nature; most grains display varying degrees of micro-faceting

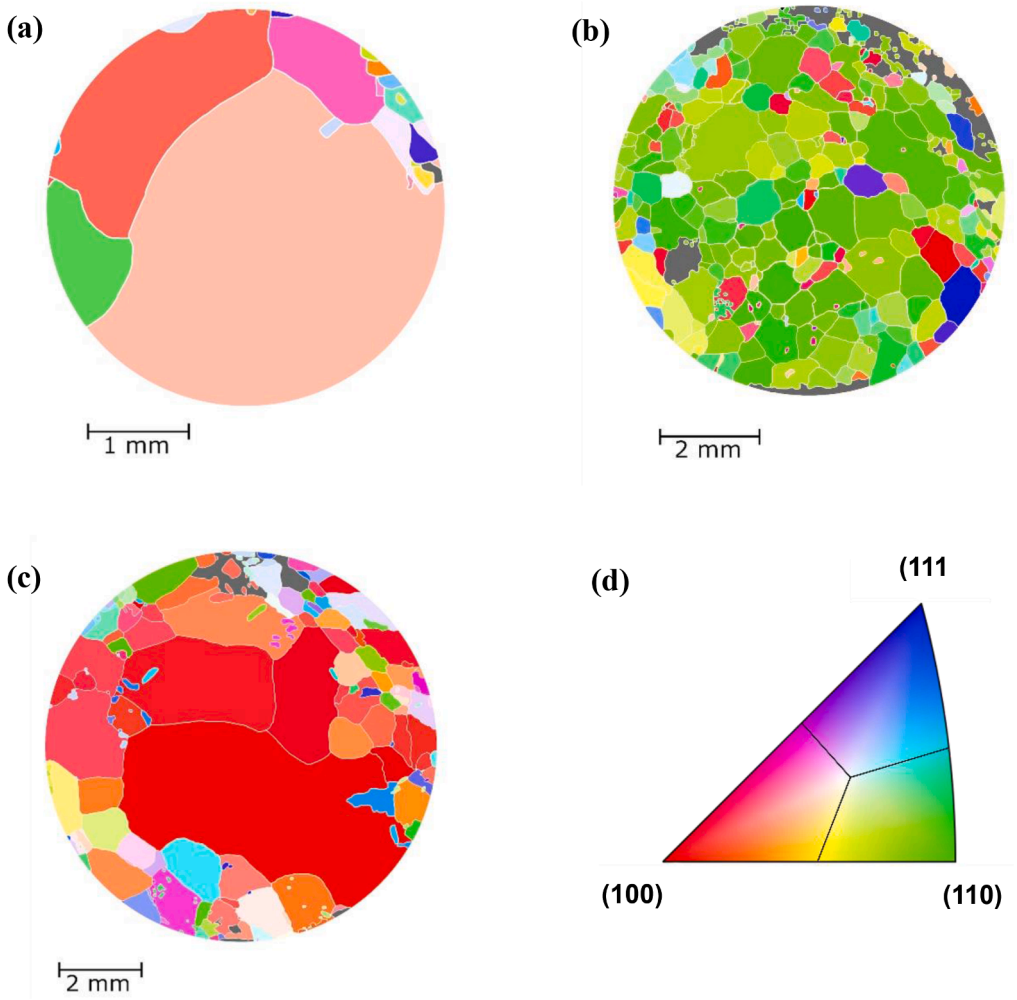

Fig. 2. Electron backscatter diffraction (EBSD) images of (a) poly_1, (b) poly_2 and (c) poly_3 with scale bars shown, where (d) is the corresponding legend consisting of a stereographic triangle colour-coded [35] according to the Pt basal planes: (111) blue, (110) green and (100) red; the overlayed black lines represent the approximate sections the stereographic triangle was divided into for assignment of the major orientation of each grain. See SI Fig. 4 for histograms of according facet distribution normalised with respect to grain size.

instead, specifically in the form of steps (following the edge of the stereographic triangle) and kinks (interior of the stereographic triangle, *i.e.*, not following the edges). Nevertheless, the EBSD measurements (Fig. 2) confirm the respective facet distributions obtained from the blank CV analysis (Fig. 1, SI Fig. 5), revealing that poly_1 and poly_3 are predominantly composed of (100)-orientated grains, whereas poly_2 is primarily (110) in nature (Fig. 2, SI Fig. 4). It should be noted, however, that the disadvantage of EBSD relative to CV in this context is that only the grain orientation can be identified easily, not the differentiation between step and terrace sites (although the step density and configuration of the steps can be calculated from EBSD maps, according to the method developed by Rupprechter et al. [36]). That is to say, where the peaks at 0.28 and 0.39 V in the blank CV of a polycrystalline Pt electrode (Fig. 1a) can be attributed to (100)-steps and (100)-terraces, respectively, the nature of the (100)-site cannot readily be distinguished using EBSD without further analysis. Therefore, a comprehensive understanding of surface structure (including both facet orientation and local coordination environment) is most readily achieved in this context by using EBSD and CV in tandem with one another.

Moreover, EBSD reveals that all three polycrystalline Pt electrodes contain only a very small proportion of (111) sites (Fig. 2), meaning that the surfaces of these electrodes are dominated by lower-coordinated facets (*i.e.*, (110) and (100)). As discussed in the introduction, this structural composition significantly complicates the interpretation of the capacitance response in the LCR. In particular, as only the (111)-facet is truly adsorbate-free in this potential window, the predominance of lower-coordinated facets implies that the majority of these electrode surfaces are covered with adsorbates in the LCR. Importantly, the different propensity for H_2O dissociation displayed by the different facets has important implications for the corresponding potential-dependent adsorbate nature, and therefore the influence on the associated capacitance response, in the LCR. More specifically, previous results suggest that the pseudo-(adsorption) capacitance associated with a potential-dependent adsorbate coverage on the (100) facet dominates the capacitance response in the LCR for stepped Pt electrodes, where only a free-charge capacitance is measured for the (111)-terraces and (110)-steps [21]. Therefore, the question remains: can we correlate the fundamental electrochemical properties (specifically the capacitance measured in the LCR region and the E_{pztc}) of these polycrystalline Pt electrodes to their respective facet distributions in spite of significant surface heterogeneity? Does our understanding of the EDL structure at model stepped Pt single crystals extend to polycrystalline Pt electrodes?

In order to determine whether this is indeed the case, the capacitance in the LCR of the three polycrystalline Pt electrodes was measured in the same 0.1 mM $HClO_4$ electrolyte for which the E_{pzfc} can be observed for Pt (111) using electrochemical impedance spectroscopy (EIS) (Fig. 3) [15, 37].

In accordance with previous findings, [3,16] the impedance response of the capacitance in the double-layer window of the three polycrystalline Pt electrodes displays constant phase element (CPE, Q) behaviour, such that a serial RQ electric equivalent circuit (EEC, where RQ refers to the solution resistance, R_s, and the double-layer capacitance, Q, respectively, connected in series with one another) was deemed more appropriate than a serial RC EEC (where C refers to an ideal capacitor) which is only appropriate for an ideally capacitive interface. Nevertheless, the deviation from ideal capacitive behaviour remained small (as quantified by the corresponding CPE exponent, α, values, SI Fig. 6, where $0.85 < \alpha < 0.95$), meaning that these Q values are close to those obtained using a perfect capacitor (where $\alpha = 1$) and/or the capacitance extracted using CV.

Regardless of the presence of CPE behaviour, significant differences in the capacitance values obtained for these respective polycrystalline Pt electrodes in the LCR region can be observed (Fig. 3). Comparing the capacitance values obtained at 0.5 V ($Q_{0.5\ V}$), the largest value ($Q_{0.5\ V}$ = 280 μF cm^{-2} $s^{\alpha-1}$) is measured for poly_3, which also contains the largest proportion of (100)-sites (Fig. 1b and 2). Poly_1, which contains a slightly smaller proportion of (100) sites, also has a correspondingly smaller $Q_{0.5\ V}$ value (240 μF cm^{-2} $s^{\alpha-1}$), whereas poly_2, which is majorly constituted of (110)-steps, has the smallest $Q_{0.5\ V}$ (110 μF cm^{-2} $s^{\alpha-1}$). Therefore, these measurements reveal that a greater proportion of (100)-facets results in a correspondingly greater capacitance in the LCR for polycrystalline Pt electrodes, suggesting that the pseudo-(adsorption) capacitance associated with (100) facets indeed dominates. These results also agree with the idea of the capacitance of individual facets being approximately additive (therefore that the overall capacitance is a weighted average of the capacitance of each of the individual grains) as modelled previously by Müller et al. for polycrystalline surfaces [38].

The marked differences in the capacitance measured in the LCR depending on the surface composition has important ramifications for the validity of the commonly used method to obtain the electrochemical

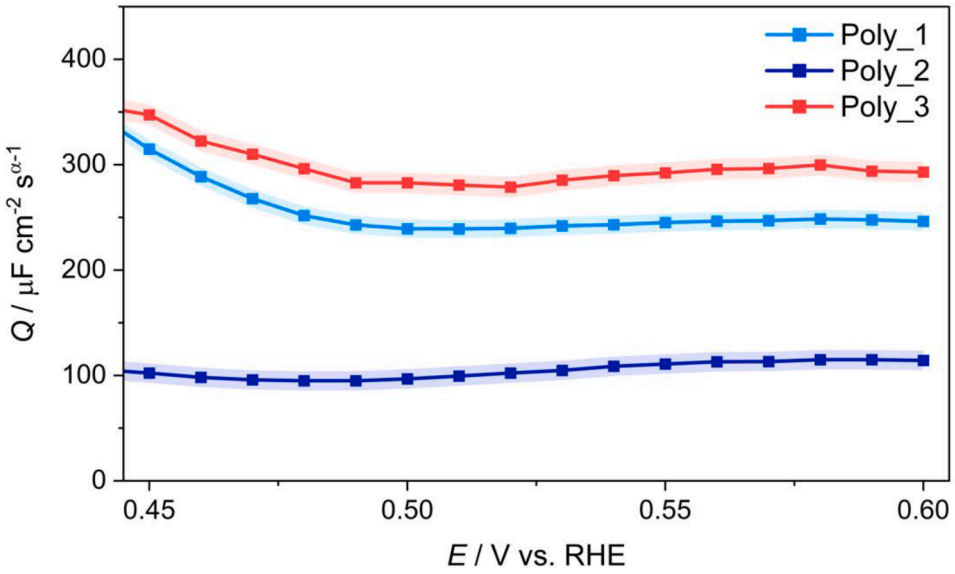

Fig. 3. Capacitance (Q) values extracted from fitting EIS data of the three polycrystalline Pt electrodes measured in 0.1 mM $HClO_4$ with a serial RQ EEC (electric equivalent circuit consisting of a resistor to model the solution resistance, R_s, and a constant phase element, Q, for the capacitance, connected in series with one another), respectively, plotted as a function of potential (ΔE = 5 mV, 10 kHz – 0.5 Hz). See SI Fig. 6 for corresponding α values. Error bars (calculated as according to SI Note 1) shown as shaded region.

surface area (ECSA) of polycrystalline Pt electrodes. Typically, the minimum in capacitance in the LCR is used as a correction factor to obtain the charge associated only with adsorption in the H_{ads} region, *i.e.*, to correct for double-layer charging effects [39]. However, as shown here and previously alluded to by Feliu et al., [1] the capacitance measured in the LCR does not correspond to a pure double-layer charging current due to the presence of pseudo-(adsorption) capacitance in the same potential window, meaning that the determination of

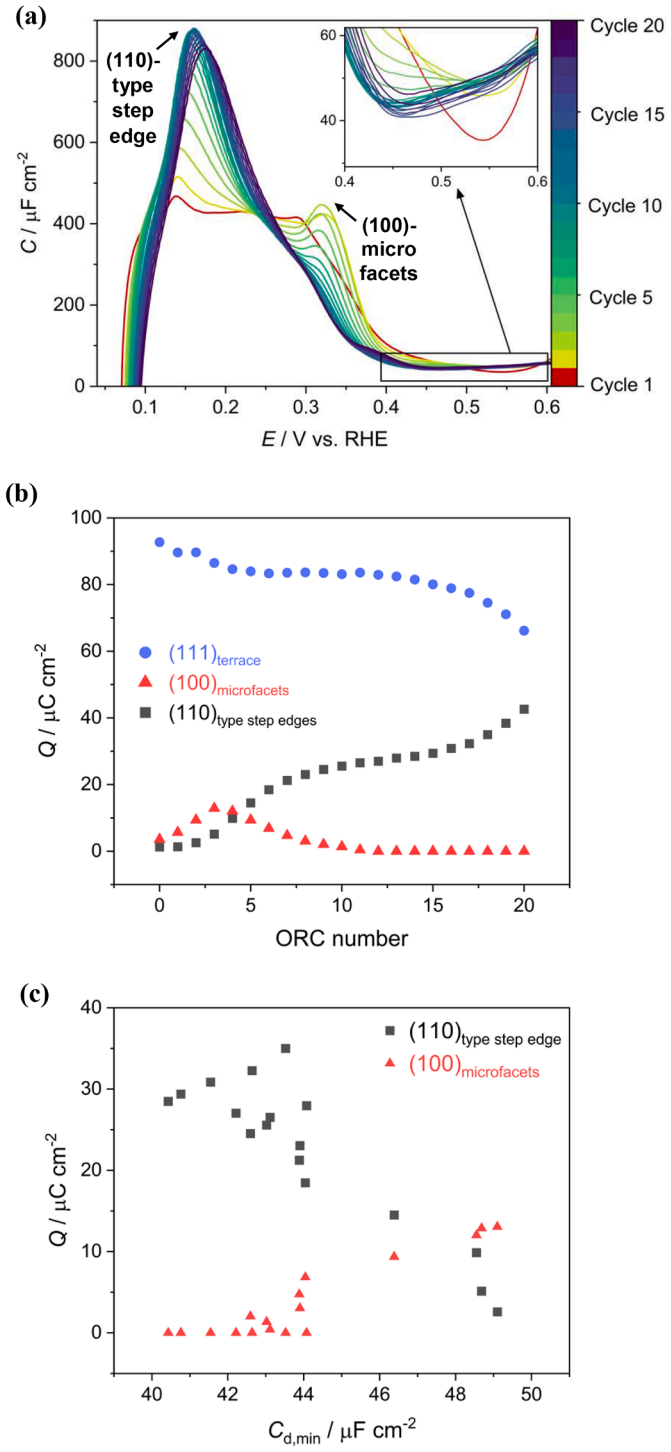

Fig. 4. (a) H_{upd} region of Pt(111) CVs in 0.1 mM $HClO_4$ after carrying out oxidation–reduction cycling (ORCs, 0.06 – 1.35 V, $\nu = 20$ mV s^{-1}, see SI Fig. 7 for full CVs) as a function of ORC number, showing the changing proportion of (110)-type step edge (referring to pure (110)-steps as well as to (110)-steps formed along a direction equivalent to [110] due to step-edge roughening) and (100)-microfacets (referring to (100)-steps at small vacancies (holes) formed in the (111) terrace and at the edges of dendritic islands) [24,41]. Inset shows the change in capacitance in the double-layer window (0.40 – 0.60 V) as a function of ORC number; (b) Integrated peak charges of the (110)-type step edge sites (black squares), (100)-microfacets (red triangles) and (111)-terrace sites (blue circles) in the H_{upd} region (obtained by peak fitting analysis carried out as according to SI Note 2; see also SI Fig. 8 for the total fit curves for exemplary ORCs), respectively, plotted as a function of ORC number; (c) Correlation plot of the integrated peak charges of (110)-type step edges and (100)-microfacets (as obtained by the peak fitting analysis, SI Note 2, SI Fig. 8) versus the minimum in capacitance in the double-layer window, $C_{d,min}$, obtained from inset in (a).

the ECSA using this method is likely not without error.

Furthermore, in order to confirm the relation between the density of (100)-sites and the capacitance measured in the LCR in a more systematic way, we also carried out oxidation–reduction cycling (ORCs) on a Pt(111) single crystal electrode. This procedure allows for the controllable formation of heterogeneous, lower-coordinated (110)- and (100)-sites that are also present on polycrystalline Pt electrodes by electrochemically roughening the Pt(111) surface [24,40]. Jacobse et al. previously quantified the structural transformations that occur during ORCs on Pt(111) using *in situ* electrochemical scanning tunnelling microscopy [24]. Of course, despite similarities in the blank voltammetry, a roughened Pt(111) surface prepared in this way cannot be considered equivalent to a polycrystalline Pt electrode surface, not only because the (110)- and (100)-defect sites conform to the edges of ad-atom and vacancy islands grown during ORCs (which differs from polycrystalline Pt in that these sites are intrinsic to the grains themselves), but also because a roughened Pt(111) surface does not contain grain boundaries which may be chemically active too. Nevertheless, carrying out ORCs on a Pt (111) surface does allow for the elucidation of a quantitative capacitance trend in the LCR as a function of different proportions of (110)- and (100)-type sites, particularly because the specific case in which the GC-capacitance minimum at the potential of zero charge, $C_{d,min}$, can be observed (0.1 mM $HClO_4$, pH 4, Fig. 4a), can be directly studied [15,37].

In agreement with the work of Jacobse et al., [24] carrying out ORCs on Pt(111) leads to marked changes in the blank voltammogram (Fig. 4a, see SI Fig. 7 for full CVs). In particular, two major changes can be observed: (i) The growth of a peak at ~0.13 V, and (ii) the initial growth and then diminution of a peak at ~0.32 V. The peak at 0.13 V was previously attributed to the growth of pure (110)-steps as well as (110)-steps formed along a direction equivalent to [110] due to step-edge roughening effects, agreeing well with the potential of (110)-steps observed in the blank voltammogram of a polycrystalline Pt electrode. Therefore, we refer to this peak at ~0.13 V as the formation of (110)-type step edges. The peak at more positive potentials (0.32 V) was previously attributed primarily to the growth of (100)-type steps formed at small vacancies (holes) on (111)-terrace sites, as well as at the edges of dendritic islands. The potential of this peak agrees well with the (100)-step peak potential on polycrystalline Pt (~0.28 V) and we will refer to it here as the formation of (100)-microfacets [24,41]. Therefore, given the close agreement with the potentials of the (110)- and (100)-step peaks for polycrystalline Pt, the (110)-type step edge and (100)-microfacet peaks present on a Pt(111) surface that has undergone ORCs can be thought of as inherently similar, which will be assumed for the following discussion.

To quantify the changing proportion of the (110)-step edge sites with respect to the (100)-microfacets (as well as the proportion of (111)-terrace sites) as a function of ORCs, we carried out a peak fitting analysis on the H_{upd} region (see SI Note 2 for more details and SI Fig. 8 for corresponding exemplary fits). From this peak fitting analysis, the charge associated with adsorption on each of these respective sites (*i.e.*, the proportion of different sites with respect to one another) could be obtained as a function of ORC number (Fig. 4b), revealing that, with increasing ORCs the proportion of (110)-type step edge sites grows continuously as a function of ORCs, oppositely mirroring the proportion of (111)-terrace sites. Contrastingly, the proportion of (100)-microfacets initially grows very rapidly, but decreases again after ~3 ORCs due to the growth and eventual coalescence of small vacancies. Therefore, after ~10 ORCs, (100)-microfacets are no longer observed (Fig. 4b).

To establish whether the proportion of the (110)-type step edge sites and (100)-microfacets are correlated to the capacitance measured in the LCR (as was found for the polycrystalline Pt electrodes), a correlation plot of the charge associated with these sites is shown in Fig. 4c as a function of $C_{d,min}$ (*i.e.*, the minimum in capacitance in the LCR, which is taken as a representative value). This analysis reveals that a larger proportion of (100)-microfacets leads to a larger $C_{d,min}$ value, which agrees well with the trends observed for the respective polycrystalline Pt electrodes (Fig. 3): A larger proportion of (100)-sites leads to a larger capacitance in the LCR. The sensitivity of $C_{d,min}$ to surface structural transformations further highlights the importance of considering this effect (see SI Fig. 9 for the changes in $C_{d,min}$ as a function of ORCs).

Furthermore, the potential of $C_{d,min}$, $E_{d,min}$, also changes markedly as a function of ORCs (Fig. 4a, SI Fig. 10a). As discussed previously, $C_{d,min}$ only corresponds to a true GC-capacitance minimum (*i.e.*, a capacitance minimum observed at the potential of zero charge, or $E_{d,min}$ in this case) for Pt(111) measured in these electrolyte conditions (at 0.54 V_{RHE} in 0.1 mM $HClO_4$) [15,37]. As soon as ORCs are carried out, or other surface heterogeneities are introduced, this is no longer the case due to pseudocapacitive surface sites, and the interpretation of the potential of this capacitance minimum, $E_{d,min}$, becomes non-trivial [42]. Importantly, however, a capacitance minimum is almost always observed in Pt electrochemistry, owing to the fact that the LCR is bordered by pseudocapacitive regions, but is often wrongly assigned to a "fundamental" $C_{d,min}$, as observed for Pt(111), *i.e.*, a measure of the E_{pzfc}. The complexity in gaining meaningful information from $E_{d,min}$ is further corroborated by the fact that $E_{d,min}$, just as $C_{d,min}$, is sensitive to structural transformations, changing significantly with ORCs carried out on Pt(111) (SI Fig. 10a). Therefore, the fundamental interpretation of $E_{d,min}$ is highly non-trivial in the presence of surface heterogeneities. A similar correlation plot of the proportion of (100)-microfacets to (110)-type step edges (in terms of their respective charges obtained by peak fitting in the H_{upd} region, Fig. 4b) with respect to $E_{d,min}$ (SI Fig. 10b), however, reveals a similar trend observed for $C_{d,min}$, *i.e.,* more (100)-sites leads to an increase in $E_{d,min}$ (albeit that this $E_{d,min}$ is always negative of the E_{pzfc} of Pt(111), in agreement with previous results on stepped Pt single crystals [21]), suggesting that there is an inherent correlation between surface structure and $E_{d,min}$.

Another key fundamental quantity pertaining to understanding the electrochemistry exhibited by heterogeneous polycrystalline Pt surfaces is the potential of zero total charge (E_{pztc}), as this reveals information about the electrosorption properties of an electrode, *i.e.*, the affinity for anion/cation adsorption as a function of potential [6]. The E_{pztc} then, by definition, should also be correlated with the facet distributions on these polycrystalline Pt surfaces as the adsorbate nature will differ depending on the facet orientation distributions as each facet itself has a different propensity for H_2O dissociation. In order to determine whether this is the case, the E_{pztc} values for the Pt basal planes in the same electrolyte conditions (0.1 mM $HClO_4$) were determined using the CO displacement technique developed by Feliu et al. [11,12] These measurements revealed significant differences in the E_{pztc} value for each Pt basal plane: Pt(110) 0.26 V < Pt(111) 0.38 V < Pt(100) 0.44 V (SI Fig. 11), corroborating the marked influence of Pt surface structure on the electrosorption properties of the respective electrode [1]. The E_{pztc} values for the three polycrystalline Pt electrodes were then obtained using the same procedure (Fig. 5).

Fig. 5 reveals that the E_{pztc} values of the three polycrystalline Pt electrodes differ markedly from one another. Plotting these E_{pztc} values in direct comparison to those obtained for the single crystal Pt basal planes in Fig. 5d reveals a direct correlation with the facet orientation distribution (obtained using CV and EBSD) and the E_{pztc} values of the respective polycrystalline Pt electrodes. More specifically, poly_2, which is primarily constituted of (110) facets (Fig. 1/2) has the most negative E_{pztc} (0.33 V, Fig. 5b), closest to the E_{pztc} of the Pt(110) basal plane (0.26 V, Fig. 5d). On the other hand, poly_1 and poly_3 (primarily (100) in nature, Fig. 1/2) have more positive E_{pztc} values of 0.39 (Fig. 5a) and 0.41 V (Fig. 5c), respectively, where poly_3 contains more (100) than poly_2 such that these E_{pztc} values are much closer to that of the Pt(100) basal plane (0.44 V, Fig. 5d). Moreover, the E_{pztc} can be roughly estimated from the weighted average of the measured relative facet distributions of each respective polycrystalline electrode [9] (in this case, obtained from EBSD data, Fig. 2, SI Fig. 4) in combination with the E_{pztc} values obtained for the Pt basal planes (SI Fig. 11, see SI Note 3/SI Table 1 for the details of this calculation). From such an analysis, the

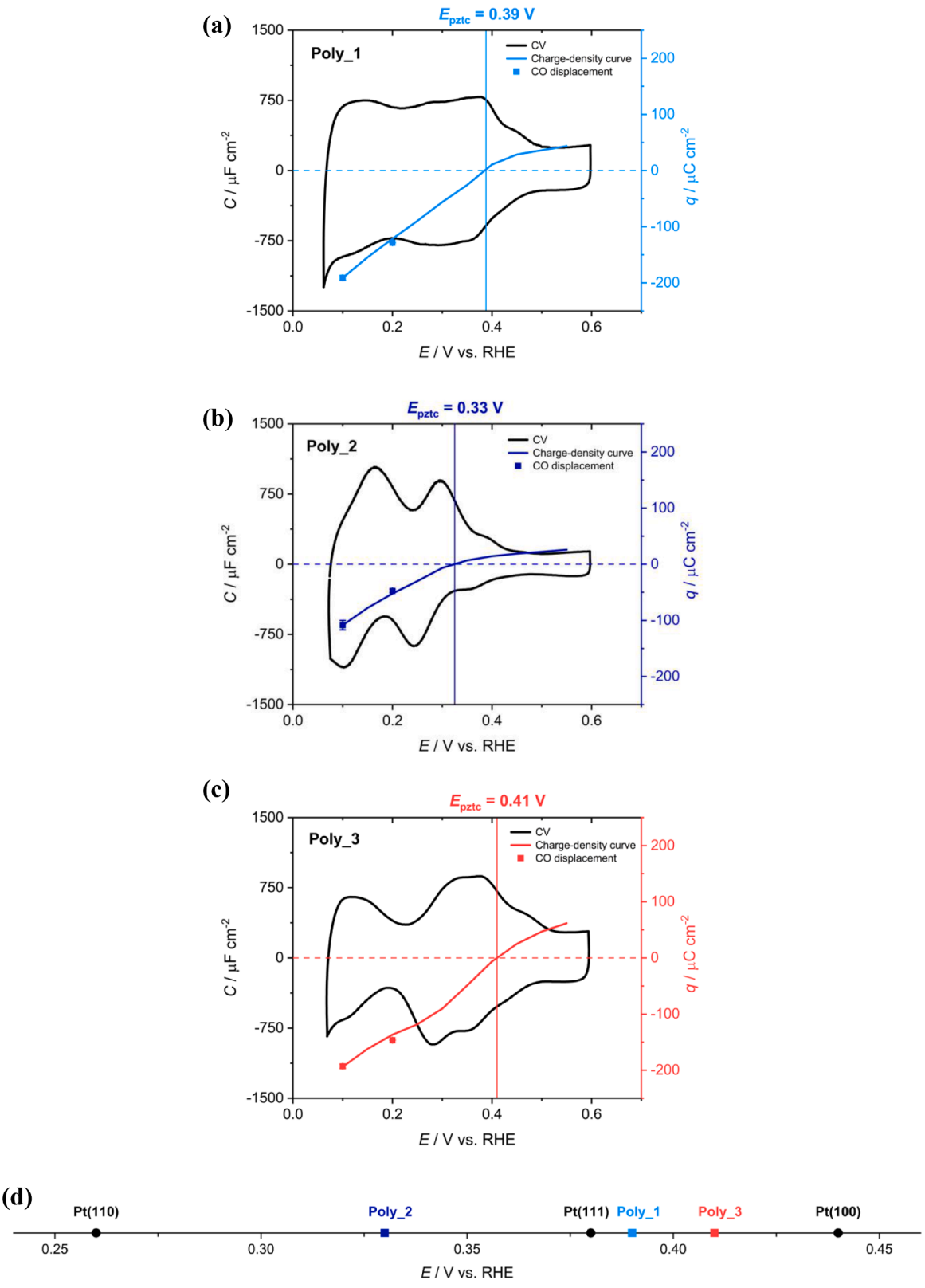

Fig. 5. CVs of three different polycrystalline Pt electrodes (a) poly_1, (b) poly_2, (c) poly_3 in 0.1 mM $HClO_4$ ($\nu = 5$ mV s^{-1}). The charge-density curve (obtained by CV integration) is shown as the coloured line (poly_1: light blue; poly_2: navy; poly_3: red) with experimental values obtained for the total charge using CO displacement plotted as markers with error bars shown (individual current transients shown in SI Fig. 13); (d) comparison of E_{pztc} values obtained for three polycrystalline Pt electrodes compared to basal plane single crystal Pt electrodes.

E_{pztc} values for poly_1, 2 and 3 are predicted to be 0.38, 0.29 and 0.39 V, respectively, in relatively close agreement with the experimentally obtained E_{pztc} values of 0.39, 0.33 and 0.41 V, respectively. Therefore, knowledge of the facet distributions as well as the E_{pztc} values of the Pt basal planes is sufficient to predict the E_{pztc} values of a polycrystalline Pt surface. Interestingly, similar results were reported by Feliu et al. for a poly-oriented single crystal Pt bead (which we define here as the case where platinum is melted and allowed to recrystallise such that no grain boundaries are formed), finding that the E_{pztc} was dictated by the facet orientations present on the surface [1]. The close agreement with the results presented in this work for polycrystalline Pt electrodes in terms of the intrinsic link between the E_{pztc} and the respective facet distributions suggests that the grain boundaries themselves are negligible in their contribution to the overall electrochemical signal (as this is the main difference in surface structure between a poly-oriented single crystal bead compared to a polycrystalline electrode).

4. Conclusion

By comparing three different polycrystalline Pt electrodes, we demonstrate, using a combination of EBSD and CV as surface characterisation techniques, that facet orientation distributions can differ markedly between electrodes. As there are significant differences in the electrochemical properties of each of the different Pt facets in terms of propensity for H_2O dissociation and catalytic activity, this work forms an imperative step towards gaining a better understanding of observed structure-capacitance relationships at a fundamental level.

Moreover, we argue that the commonly coined "double-layer" region between 0.40 – 0.60 V_{RHE} in $HClO_4$ electrolyte for Pt electrodes is misleading terminology due to a non-trivial adsorbate coverage for all Pt facets other than Pt(111) in this potential window. Instead, we propose the term "low capacitance region" (LCR). Importantly, we show that a larger proportion of (100)-facets on the polycrystalline Pt surface leads to a significant increase in capacitance in the LCR, consistent with the trends observed previously for (100)-stepped Pt single crystal electrodes. This suggests that the pseudo-(adsorption) capacitance associated with a potential-dependent changing adsorbate coverage on (100)-sites indeed dominates the capacitance response in the LCR. These trends were corroborated more systematically by carrying out ORCs on Pt(111), where the structural transformations have been well elucidated.

Furthermore, we reveal that the E_{pztc} value obtained by CO displacement agrees well with the predicted value calculated from the weighted average of the respective facet orientation distribution, in turn suggesting that the fundamental electrochemical properties of a polycrystalline Pt electrode can be predicted in spite of a complex surface structure and the presence of grain boundaries (see SI Fig. 14 where the interdependence between facet distributions and the capacitance in the LCR/E_{pztc} can be observed).

In conclusion, our findings establish a direct correlation between the surface structure (facet orientation distribution) of polycrystalline Pt electrodes and their fundamental electrochemical properties, particularly the capacitance in the LCR and potential of zero total charge. These insights extend our novel understanding of the structure-sensitivity of the double-layer properties observed for model stepped single crystal Pt electrodes to more complex polycrystalline surfaces.

Data availability

Data will be made available on request.

Declaration of competing interest

The authors declare that they have no known competing financial interests or personal relationships that could have appeared to influence the work reported in this paper.

Acknowledgements

NLF and MTMK received funding from the European Research Council (ERC) (advanced grant no. 101019998 "FRUMKIN"). HS received funding from the Swedish Research Council (project 2021–05846).

Supplementary materials

Supplementary material associated with this article can be found, in the online version, at doi:10.1016/j.electacta.2025.147977.

References

[1] Q.-S. Chen, J. Solla-Gullón, S.-G. Sun, J.M. Feliu, The potential of zero total charge of Pt nanoparticles and polycrystalline electrodes with different surface structure: the role of anion adsorption in fundamental electrocatalysis, Electrochim. Acta 55 (2010) 7982–7994.
[2] K.J.J. Mayrhofer, et al., The impact of geometric and surface electronic properties of Pt-catalysts on the particle size effect in electrocatalysis, J. Phys. Chem. B 109 (2005) 14433–14440.
[3] K.-T. Song, et al., Influence of the electrolyte pH on the double layer capacitance of polycrystalline Pt and Au electrodes in acidic solutions, ChemElectroChem 12 (2025) e202400587.
[4] Bockris, J.O.M., Conway, B.E. & Yeager, E. Comprehensive Treatise of Electrochemistry. (New York, 1980).
[5] M.J. Weaver, Potentials of zero charge for platinum(111)−aqueous interfaces: A combined assessment from In-situ and ultrahigh-vacuum measurements, Langmuir 14 (1998) 3932–3936.
[6] A.N. Frumkin, O.A. Petrii, Potentials of zero total and zero free charge of platinum group metals, Electrochim. Acta 20 (1975) 347–359.
[7] V. Climent, G.A. Attard, J.M. Feliu, Potential of zero charge of platinum stepped surfaces: a combined approach of CO charge displacement and N_2O reduction, J. Electroanal. Chem. 532 (2002) 67–74.
[8] L.F. Gaudin, M. Kang, C.L. Bentley, Facet-dependent electrocatalysis and surface electrochemical processes on polycrystalline platinum, Electrochim. Acta 450 (2023) 142223.
[9] Y. Wang, E. Gordon, H. Ren, Mapping the potential of zero charge and electrocatalytic activity of metal–Electrolyte interface via a grain-by-grain approach, Anal. Chem. 92 (2020) 2859–2865.
[10] J.T. Bender, et al., The potential of zero total charge predicts cation effects for the oxygen reduction reaction, ACS Energy Lett. 9 (2024) 4724–4733.
[11] V. Climent, R. Gómez, J.M. Feliu, Effect of increasing amount of steps on the potential of zero total charge of Pt(111) electrodes, Electrochim. Acta 45 (1999) 629–637.
[12] J. Clavilier, et al., Study of the charge displacement at constant potential during CO adsorption on Pt(110) and Pt(111) electrodes in contact with a perchloric acid solution, J. Electroanal. Chem. 330 (1992) 489–497.
[13] A.J. Bard, L.R. Faulkner, Electrochemical Methods Fundamentals and Applications, John Wiley & Sons, Inc., 2001.
[14] M.T.M. Koper, Structure sensitivity and nanoscale effects in electrocatalysis, Nanoscale 3 (2011) 2054–2073.
[15] K. Ojha, N. Arulmozhi, D. Aranzales, M.T.M. Koper, Double layer at the Pt(111)–Aqueous electrolyte interface: potential of zero charge and anomalous gouy–Chapman screening, Angew. Chem. Int. Ed. 59 (2020) 711–715.
[16] N.L. Fröhlich, J.J.J. Eggebeen, M.T.M. Koper, Measurement of the double-layer capacitance of Pt(111) in acidic conditions near the potential of zero charge, Electrochim. Acta 494 (2024) 144456.
[17] R. Rizo, et al., Analysis of the OH coverage on low-coordinated Pt sites at low potentials, ACS Electrochemistry (2024) 351–359.
[18] R. Rizo, et al., Investigating the presence of adsorbed species on Pt steps at low potentials, Nat. Commun. 13 (2022) 2550.
[19] X. Chen, I.T. McCrum, K.A. Schwarz, M.J. Janik, M.T.M. Koper, Co-adsorption of cations as the cause of the apparent pH dependence of hydrogen adsorption on a stepped platinum single-crystal electrode, Angew. Chem. Int. Ed. 56 (2017) 15025–15029.
[20] O. Diaz-Morales, T.J.P. Hersbach, C. Badan, A.C. Garcia, M.T.M. Koper, Hydrogen adsorption on nano-structured platinum electrodes, Faraday Discuss 210 (2018) 301–315.
[21] N.L. Fröhlich, et al., A comprehensive model for the electric double layer of stepped platinum electrodes. Accepted, Nature Chem. (2025).
[22] N. Fröhlich, et al., Effect of trace impurities in perchloric acid on blank voltammetry of Pt(111), Electrochim. Acta 466 (2023) 143035.
[23] W. Schmickler, E. Santos, Interfacial Electrochemistry, Springer, 2010.
[24] L. Jacobse, M.J. Rost, M.T.M Koper, Atomic-scale identification of the electrochemical roughening of platinum, ACS Cent. Sci. 5 (2019) 1920–1928.
[25] J. Clavilier, The role of anion on the electrochemical behaviour of a {111} platinum surface; an unusual splitting of the voltammogram in the hydrogen region, J. Electroanal. Chem Interfacial Electrochem. 107 (1980) 211–216.
[26] J. Clavilier, R. Faure, G. Guinet, R. Durand, Preparation of monocrystalline Pt microelectrodes and electrochemical study of the plane surfaces cut in the direction

of the {111} and {110} planes, J. Electroanal. Chem. Interfacial Electrochem. 107 (1980) 205–209.
[27] T. Omori, et al., Abnormal grain growth induced by cyclic heat treatment, Science (1979) 341 (2013) 1500–1502.
[28] G.A. Attard, et al., The voltammetry of surfaces vicinal to Pt{110}: structural complexity simplified by CO cooling, J. Electroanal. Chem. 793 (2017) 137–146.
[29] L.A. Kibler, A. Cuesta, M. Kleinert, D.M. Kolb, In-situ STM characterisation of the surface morphology of platinum single crystal electrodes as a function of their preparation, J. Electroanal. Chem. 484 (2000) 73–82.
[30] R. Rizo, E. Herrero, V. Climent, Juan.M. Feliu, On the nature of adsorbed species on Platinum Single Crystal electrodes, Curr. Opin. Electrochem. 38 (2023) 101240.
[31] F.J. Vidal-Iglesias, R.M. Arán-Ais, J. Solla-Gullón, E. Herrero, J.M. Feliu, Electrochemical characterization of shape-controlled Pt nanoparticles in different supporting electrolytes, ACS Catal. 2 (2012) 901–910.
[32] J. Solla-Gullón, P. Rodríguez, E. Herrero, A. Aldaz, J.M. Feliu, Surface characterization of platinum electrodes, Phys. Chem. Chem. Phys. 10 (2008) 1359–1373.
[33] X. Chen, K. Ojha, M.T.M. Koper, Deconvolution of the voltammetric features of a Pt (100) single-crystal electrode, J. Phys. Chem. Lett. 15 (2024) 4958–4964.
[34] F.V. Mascaró, M.T.M. Koper, M.J. Rost, Quantitative study of electrochemical adsorption and oxidation on Pt(111) and its vicinal surfaces, Electrochim. Acta 506 (2024) 145014.
[35] D.N. Johnstone, B.H. Martineau, P. Crout, P.A. Midgley, A.S. Eggeman, Density-based clustering of crystal (mis)orientations and the orix Python library, J. Appl. Crystallogr. 53 (2020) 1293–1298.
[36] P. Winkler, et al., How the anisotropy of surface oxide formation influences the transient activity of a surface reaction, Nat. Commun. 12 (2021) 69.
[37] K. Ojha, K. Doblhoff-Dier, M.T.M. Koper, Double-layer structure of the Pt(111)–aqueous electrolyte interface, Proc. Natl. Acad. Sci. U. S. A. 119 (2022) e2116016119.
[38] R. Müller, J. Fuhrmann, M. Landstorfer, Modeling polycrystalline electrode-electrolyte interfaces: the differential capacitance, J. Electrochem. Soc. 167 (2020) 106512.
[39] S. Trasatti, O.A. Petrii, Real surface area measurements in electrochemistry, Pure Appl. Chem. 63 (1991) 711–734.
[40] A.M. Gómez-Marín, J.M. Feliu, Pt(111) surface disorder kinetics in perchloric acid solutions and the influence of specific anion adsorption, Electrochim. Acta 82 (2012) 558–569.
[41] F. Valls Mascaró, I.T. McCrum, M.T.M. Koper, M.J. Rost, Nucleation and growth of dendritic islands during platinum oxidation-reduction cycling, J. Electrochem. Soc. 169 (2022) 112506.
[42] N.L. Fröhlich, M.T.M. Koper, Progress and pitfalls in measuring the double-layer capacitance of platinum electrodes, Curr. Opin. Electrochem. 53 (2025) 101727.